S-parameter Reciprocity Relations, Normalization, and TLR Error Box Completion

S. Vandenberghe, D. Schreurs, G. Carchon*,
B. Nauwelaers, W. De Raedt*

K.U.Leuven ESAT TELEMIC, Kasteelpark Arenberg 10, B–3001 Leuven, Belgium
*IMEC MCP, Kapeldreef 75, B–3001 Leuven, Belgium

The following preprint differs from the final publication:

S. Vandenberghe, D. Schreurs, G. Carchon, B. Nauwelaers, W. De Raedt, "*S*-parameter Reciprocity Relations, Normalization, and TLR Error Box Completion," *Int J RF and mm-wave CAE,* John Wiley & Sons, Inc., vol. 12, no. 5, 2002, pp. 418–427.

S-parameter Reciprocity Relations, Normalization, and TLR Error Box Completion

S. Vandenberghe, D. Schreurs, G. Carchon*,
B. Nauwelaers, W. De Raedt*

K.U.Leuven ESAT TELEMIC, Kasteelpark Arenberg 10, B–3001 Leuven, Belgium
*IMEC MCP, Kapeldreef 75, B–3001 Leuven, Belgium

Index Terms— Microwave measurements, calibration, coplanar waveguides.

Abstract— The condition imposed by the Lorentz reciprocity theorem, a field property, on microwave circuit parameters is derived. The effect of power consistency and renormalization is discussed. A robust multi-reflect Thru-Line-Reflect error box completion scheme is presented. The relative calibration is then converted into an absolute calibration using error box reciprocity.

1 Introduction

Reciprocity of a two-port junction is a necessary condition for the determination of the forward and reverse transmission if only their product is known, as obtained from e.g. SOL or TLR calibration techniques. Equating both quantities[1, p. 159] is not always valid as shown in [2]. An absolute determination requires power meters and phase standards, which are not readily available for e.g. coax to coplanar waveguide junctions.

The condition reciprocity imposes on the microwave circuit parameters depends on the underlying field phenomenon and on the normalization, which relates the field with the voltage and current. This paper decouples reciprocity and normalization. It also shows that power consistency, between the field and the circuit parameters, simplifies the reciprocity relation for most practical junctions. Formulas valid for any normalization are developed and the reciprocity ratio S_{21}/S_{12} for Marks' traveling wave intensities[2] is recalculated.

TLR employs two transmission lines and two equal reflects for the determination of the 7-term error model. From the thru-line data follows[3] the line propagation constant and two relations per error box. The calibration is completed via the thru S-parameters and one equation from the reflect measurement. The standard algorithm[4] uses the error box reflection's reciprocal, $1/S_{x22}$, which is undefined if S_{x22} is zero up to measurement precision. Spike errors may appear when sequencing calibration comparison, e.g. when modelling a capacitor via TLR.

The here presented algorithm completes the error boxes using its transmission coefficients. Requiring non-zero transmission does not introduce a deficiency since this is essential for any deembedding technique. All intermediate results are bounded, well defined, and approach a constant value for the ideal case. Moreover, the calculation sequence exploits the problem symmetry and aims for robustness. Redundant data is explicitly demonstrated, allowing for a real time error estimate. The algorithm is further extended to include Line-Reflect-Match and the zero- and multi-reflect case. Finally, the 8-term absolute error model is computed assuming reciprocity.

2 Reciprocity

A voltage current, or voltage S-parameter, circuit representation is a compact way of describing a field problem. This equivalence is possible if the field components of the incident and reflected wave are either in phase or in counter-phase. The fields at port i thus satisfy

$$\begin{aligned}[\vec{E}_i, \vec{H}_i] &= [\vec{e}_{ti} + \vec{e}_{zi}, \vec{h}_{ti} + \vec{h}_{zi}] C_{0i}^{+} e^{-\gamma_i z} \\ &\quad + [\vec{e}_{ti} - \vec{e}_{zi}, -\vec{h}_{ti} + \vec{h}_{zi}] C_{0i}^{-} e^{\gamma_i z} \end{aligned} \quad (1)$$

with $\vec{e}, \vec{h}$ the z-independent modal fields and C_0^+, C_0^- the two wave amplitude constants. A normalization relates the transverse components $\vec{e}_t, \vec{h}_t$ with V_c, I_c, the modal voltage and current, and sets the characteristic line impedance. The wave voltages at port i, V_0^+ and V_0^-, determine the fields since

$$C_{0i}^{\pm} = \frac{V_{0i}^{\pm}}{V_{ci}} = \frac{I_{0i}^{\pm}}{I_{ci}} \quad \Rightarrow \quad Z_{ci} = \frac{V_{ci}}{I_{ci}} = \frac{V_{0i}^{+}}{I_{0i}^{+}} = \frac{V_{0i}^{-}}{I_{0i}^{-}} \quad (2)$$

holds from (1). An arbitrary transversal field then follows from[1, p. 146]

$$\vec{E}_{ti} = \left(\frac{V_{0i}^{+}}{V_{ci}} e^{-\gamma_i z} + \frac{V_{0i}^{-}}{V_{ci}} e^{\gamma_i z} \right) \vec{e}_{ti} = \frac{V_i(z)}{V_{ci}} \vec{e}_{ti} \quad (3)$$

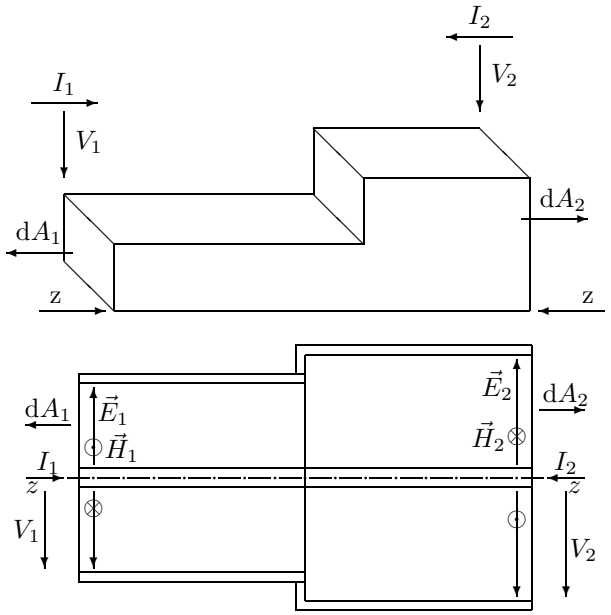

Figure 1: Examples of reciprocal microwave circuits. Top: A TE_{10} E-plane step rectangular waveguide junction. Bottom: A TM dissimilar coaxial transmission line junction.

$$\vec{H}_{ti} = \left(\frac{I_{0i}^{+}}{I_{ci}}e^{-\gamma_i z} - \frac{I_{0i}^{-}}{I_{ci}}e^{\gamma_i z}\right)\vec{h}_{ti} = \frac{I_i(z)}{I_{ci}}\vec{h}_{ti} \quad (4)$$

with V and I the port voltage and current.

The Lorentz reciprocity theorem[1, pp. 57–59, 159] applied on a two-port source free junction, e.g. fig. 1, imposes a condition on the incident and reflected field. The Lorentz integral

$$\oint_A (\vec{E}^I \times \vec{H}^{II} - \vec{E}^{II} \times \vec{H}^I)\mathrm{d}\vec{A} = 0 \quad (5)$$

over the junction enclosing surface A reduces to the two terminal planes if the remaining surface is perfectly conducting, characterized by a scalar surface impedance, or is infinitely far away. Substituting the fields in terms of (1) relates the wave amplitudes. The integrand simplifies to the transverse components if $\vec{e}_t, \vec{h}_t$ are parallel, and if $\vec{e}_z, \vec{h}_z$ are normal, to the terminal plane. TE and TM waves[1, p. 72] satisfy this condition. Choosing sources outside of the junction such that $\vec{E}_{t2}^I = 0$, experiment I, and such that $\vec{E}_{t1}^{II} = 0$, experiment II, with (3–4) gives

$$\frac{V_2^{II} I_2^I}{V_1^I I_1^{II}} = \frac{\frac{1}{V_{c1}I_{c1}}\int_{A_1} \vec{e}_{t1} \times \vec{h}_{t1}\mathrm{d}\vec{A}}{\frac{1}{V_{c2}I_{c2}}\int_{A_2} \vec{e}_{t2} \times \vec{h}_{t2}\mathrm{d}\vec{A}} \quad (6)$$

or with the reciprocity factor

$$K_i = \frac{1}{V_{ci}I_{ci}}\int_{A_i} \vec{e}_{ti} \times \vec{h}_{ti} \cdot \vec{u}_z \mathrm{d}A \quad (7)$$

and (2) in

$$\frac{Y_{21}}{Y_{12}} = \frac{K_1}{K_2} \quad \Leftrightarrow \quad D = \frac{S_{21}}{S_{12}} = \frac{Z_{c2}K_1}{Z_{c1}K_2} \quad (8)$$

which agrees with [2, eq. 22]. The S-parameter reciprocity ratio D alternatively follows from (5) with port 2/1, experiment I/II, matched. A good choice of V_c, I_c sets K to unity and implies

$$\arg(K_i) = 0 \quad \Leftrightarrow \quad \arg(V_{ci}I_{ci}) = \arg(\vec{e}_{ti}\vec{h}_{ti}) \quad (9)$$

if the phase of the transverse field is constant in the terminal plane, e.g. for TE and TM waves.

3 Power consistency

The power transmitted across port i follows from

$$S_t = \frac{1}{2}\int_A \vec{E}_t \times \vec{H}_t^* \cdot \vec{u}_z \mathrm{d}A \quad (10)$$

if the transverse components are parallel, and the axial components normal, to the terminal plane. Substituting (3–4) and defining the modal power

$$S_c = \frac{1}{2}\int_A \vec{e}_t \times \vec{h}_t^* \cdot \vec{u}_z \mathrm{d}A\,, \quad (11)$$

the power carried by the forward modal field, yields

$$S_t = \frac{VI^*}{V_c I_c^*} S_c = (C^+ + C^-)(C^+ - C^-)^* S_c \quad (12)$$

which agrees with the circuit power $\frac{1}{2}VI^*$ only if

$$S_c = \frac{1}{2}\int_A \vec{e}_t \times \vec{h}_t^* \cdot \vec{u}_z \mathrm{d}A = \frac{1}{2}V_c I_c^* \quad (13)$$

holds. From this power consistency follows

$$Z_c = \frac{V_c}{I_c} = \frac{|V_c|^2}{2S_c^*} = \frac{2S_c}{|I_c|^2} = \frac{\int_A Z_w \vec{h}_t \vec{h}_t^* \mathrm{d}A}{|I_c|^2}\,, \quad (14)$$

uniquely determining the phase of Z_c[5], and

$$\arg\left(\frac{2S_c}{V_c I_c^*}\right) = 0 \quad \Leftrightarrow \quad \arg(V_c I_c^*) = \arg(\vec{e}_t \vec{h}_t^*) \quad (15)$$

if the modal field's phase is constant in the terminal plane. If V_c is in phase with $\vec{e}_t$ or if I_c is in phase with $\vec{h}_t$, e.g. defined by a path integral for TM waves or by a contour integral for TE waves, then (9) holds from (15), and $K = 1$ follows from (13). Converse, (9) and (15) can only be satisfied if the modal voltage and current are in phase with their corresponding field component. In general, if two out of the four conditions

$$\begin{array}{ll} \arg(K) = 0 & \arg\left(\frac{2S_c}{V_c I_c^*}\right) = 0 \\ \arg(V_c) = \arg(\vec{e}_t) & \arg(I_c) = \arg(\vec{h}_t) \end{array} \quad (16)$$

are satisfied, then the remaining conditions hold and

$$K = 1 \quad \Leftrightarrow \quad \frac{2S_c}{V_c I_c^*} = 1 \tag{17}$$

follows. Requiring a unit reciprocity factor and power consistency thus uniquely determines the phase of the modal voltage and current. A good definition has one degree of freedom, the magnitude $|V_c|$ or $|I_c|$, proportional to the modal field, or the magnitude $|Z_c|$.

4 Renormalization

The two wave voltages V^+, V^- at port i can be scaled by a constant. A good choice may simplify the reciprocity relation (8) or may set $|V_n^+|^2/2$ equal to the true power. The renormalized V_c, I_c follow from

$$V_{cni} = \frac{V_{ci}}{k_{vi}} \qquad I_{cni} = k_{ii} I_{ci} \tag{18}$$

which scales

$$V_{ni}^{\pm} = \frac{V_i^{\pm}}{k_{vi}} \qquad I_{ni}^{\pm} = k_{ii} I_i^{\pm} \tag{19}$$

and yields the normalized quantities

$$K_{ni} = \frac{V_{ci} I_{ci}}{V_{cni} I_{cni}} K_i = \frac{k_{vi}}{k_{ii}} K_i \tag{20}$$

$$Z_{cni} = \frac{V_{cni}}{I_{cni}} = \frac{Z_{ci}}{k_{vi} k_{ii}} \tag{21}$$

$$S_{cni} = \frac{1}{2} V_{cni} I_{cni}^* = \frac{k_{ii}^*}{k_{vi}} S_{ci} \tag{22}$$

$$\frac{Z_{cni}}{K_{ni}} = \frac{1}{k_{vi}^2} \frac{Z_{ci}}{K_i} \tag{23}$$

$$S_{nji} = \frac{k_{vi}}{k_{vj}} S_{ji} \tag{24}$$

$$D_{nji} = \frac{k_{vi}^2}{k_{vj}^2} \frac{Z_{cj} K_i}{Z_{ci} K_j} \tag{25}$$

with D_n the normalized reciprocity ratio. Conservation of reciprocity (20) and modal power (22) for the normalized voltage and current requires a real scale factor $k_v = k_i$.

Collin[1, p. 173] chooses $k_v = \sqrt{Z_c}$ and implicitely sets $k_i = k_v$. This conserves reciprocity, transforms the characteristic impedance to unity and reduces the power to the apparent power. Setting $k_i = k_v^*$ maintains the power equivalence but results in a non-standard reciprocity condition, see table 1. The normalized admittance matrix cannot describe the circuit unless Z_c is real.

These voltage normalized S-parameters remove the Z_c dependence of the reciprocity ratio. D_n becomes

$$D_n = \frac{S_{n21}}{S_{n12}} = \frac{Z_{cn2}/K_{n2}}{Z_{cn1}/K_{n1}} = \frac{S_{21}\sqrt{\frac{Z_{c1}}{Z_{c2}}}}{S_{12}\sqrt{\frac{Z_{c2}}{Z_{c1}}}} = \frac{K_1}{K_2}. \tag{26}$$

$k_{vi} = \sqrt{Z_{ci}}$	$k_{ii} = k_{vi}$	$k_{ii} = k_{vi}^*$
$Y_{21} = Y_{12} \Rightarrow$	$\frac{Y_{n21}}{Y_{n12}} = 1$	$\frac{Y_{n21}}{Y_{n12}} = \sqrt{\frac{Z_{c1} Z_{c2}^*}{Z_{c1}^* Z_{c2}}}$
$S_{cni} =$	$\lvert S_{ci} \rvert$	S_{ci}
$Z_{cni} =$	1	$\sqrt{Z_{ci}/Z_{ci}^*}$
$\frac{\lvert V_{ni}^+ \rvert^2}{2Z_{cni}} =$	$\frac{\lvert V_i^+ \rvert^2}{2\lvert Z_{ci} \rvert}$	$\frac{\lvert V_i^+ \rvert^2}{2Z_{ci}}$

Table 1: The effect of the choice of k_i, when normalizing with $k_v = \sqrt{Z_c}$, on reciprocity, modal power, characteristic impedance and the power in a forward propagating wave. Left: reciprocity conservation. Right: power conservation

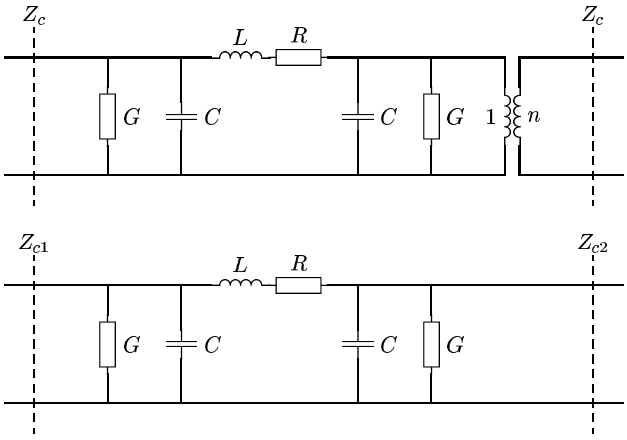

Figure 2: Typical equivalent circuits modelling reciprocal junctions. Top: The line impedance Z_c of a waveguide is usually chosen equal to the wave impedance Z_w. The step geometry difference is modelled by a voltage change. Bottom: Voltage continuity is typical for an ideal coaxial line junction. The geometry change yields a different line impedance. The normalized S-parameters coincide if $n = \sqrt{Z_{c1}/Z_{c2}}$.

Also, the normalized wave voltages are independent of a real prescaling factor, as follows from

$$\begin{cases} V_{cr} = \frac{V_c}{k_r} \\ I_{cr} = I_c k_r \end{cases} \quad \Rightarrow \quad \begin{cases} V_{cn} = \frac{V_{cr}}{\sqrt{Z_{cr}}} = \frac{V_c}{\sqrt{Z_c}} \\ I_{cn} = I_{cr}\sqrt{Z_{cr}} = I_c\sqrt{Z_c} \end{cases} \tag{27}$$

Thus, any good definition (16–17) of V_c and I_c for TE or TM waves yields the same normalized values, independent of the actual $|V_c|$, $|I_c|$ or $|Z_c|$. Moreover, K and D_n are then unity. The field follows from

$$C_i^{\pm} = \frac{V_i^{\pm}}{V_{ci}} = \frac{V_{ni}^{\pm}\sqrt{Z_{ci}}}{V_{ci}} = \frac{V_{ni}^{\pm}}{\sqrt{V_{ci} I_{ci}}} \tag{28}$$

with the denominator known from the modal solution.

Converse, a circuit interpretation of voltage normalized S-parameters requires an external estimate of $|V_c|$, $|I_c|$ or $|Z_c|$. The line impedance Z_c of a waveguide is usually chosen equal to the wave impedance,

which is constant over e.g. the E-plane step in fig. 1. The modal voltage at each port follows from power consistency[1, p. 162] (14), and depends on the waveguide height. For coaxial lines, the modal voltage V_c is best defined using a path integral in the terminal plane between the two conductors. This guarantees voltage continuity over an ideal junction and defines Z_c. Figure 2 shows typical equivalent circuits.

A relative calibration like SOL recovers the junction's S_{11}, S_{22} and $S_{21}S_{12}$. Reciprocity is often used to normalize the S-parameters. Thus,

$$S_{r,sol} \approx \begin{bmatrix} S_{11} & kS_{12} \\ S_{21}/k & S_{22} \end{bmatrix}, \quad (29)$$

with k unknown, is usually normalized through

$$S_{n21} = S_{n12} = \sqrt{S_{r21}S_{r12}} \quad \Leftrightarrow \quad k = \sqrt{\frac{S_{21}}{S_{12}}} \quad (30)$$

setting $D_n = 1$ and implicitely choosing

$$k_{vi} = \sqrt{\frac{Z_{ci}}{K_i}} \quad (31)$$

which coincides with the voltage normalized S-parameters if K is unity. The absolute on-wafer calibration of Agilent's Non-linear Network Measurement System uses this property. First, a SOL calibration between the probe port 2 and an auxiliary coax port b is performed[6]. Second, a power meter measures $|V_b^-|$ for a V_2^+. Third, a phase standard excites V_b^+ and V_2^- is measured. The absolute voltage waves at the probe follow from

$$\begin{bmatrix} V_2^- \\ V_2^+ \end{bmatrix} \sqrt{\frac{K_2}{Z_{c2}}} = T_n \begin{bmatrix} V_b^+ \\ V_b^- \end{bmatrix} \sqrt{\frac{K_b}{Z_{cb}}} \quad (32)$$

with T_n the normalized cascading wave matrix, Z_{c2} the on wafer line impedance and Z_{cb} the coaxial line impedance. This scaling is avoided by setting Z_{c2} equal to Z_{cb} before the absolute calibration, and assuming a unity reciprocity factor.

Marks defines two traveling wave intensities as

$$V_n^\pm = \sqrt{2\Re(S_c)}\frac{V^\pm}{V_c} = \frac{|V_c|\sqrt{\Re(Z_c)}}{|Z_c|V_c}V^\pm \quad (33)$$

with the property that $|V_n^+|^2/2$ equals the true power, if all voltages are defined as peak values. Substituting k_v from above in equation (23) yields

$$\frac{Z_{cn}}{K_n} = \frac{1}{\frac{Z_c}{|V_c|^2}\int \vec{e}_t \times \vec{h}_t \cdot \vec{u}_z \mathrm{d}A} \cdot \frac{1}{1 - j\frac{\Im(Z_c)}{\Re(Z_c)}} \quad (34)$$

from which D_n follows, equal to [2, eq. 21].

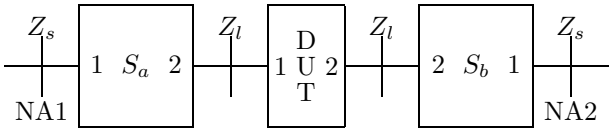

Figure 3: The TLR error box port numbering. The port 2 reference impedance is set by the line impedance Z_l.

5 TLR error box completion

From the thru-line measurement data follows an estimate of the line propagation constant γ and

$$\alpha_a \approx S_{a11} \qquad \beta_a \approx \frac{S_{a22}}{\det(S_a)} \quad (35)$$

for error box a, see [3]. The here introduced port numbering, fig. 3, takes advantage of the problem symmetry. The relations for box $x = [a, b]$ become

$$\alpha_x \approx S_{x11} \qquad \chi_x = \frac{\beta_x}{\beta_x\alpha_x - 1} \approx \frac{S_{x22}}{S_{x21}S_{x12}}. \quad (36)$$

The thru or line data gives

$$c_a = S_{t11} - \alpha_a \approx \frac{S_{a21}S_{a12}e^{-2\gamma l}S_{b22}}{1 - S_{a22}e^{-2\gamma l}S_{b22}} \quad (37)$$

$$S_{t12} \approx \frac{S_{b21}e^{-\gamma l}S_{a12}}{1 - S_{a22}e^{-2\gamma l}S_{b22}} \quad (38)$$

$$S_{t21} \approx \frac{S_{a21}e^{-\gamma l}S_{b12}}{1 - S_{a22}e^{-2\gamma l}S_{b22}} \quad (39)$$

$$c_b = S_{t22} - \alpha_b \approx \frac{S_{b21}S_{b12}e^{-2\gamma l}S_{a22}}{1 - S_{a22}e^{-2\gamma l}S_{b22}} \quad (40)$$

and allows the calculation of e, p via

$$e = \frac{1}{2}\left(\frac{\chi_a c_a}{\chi_a c_a + 1} + \frac{\chi_b c_b}{\chi_b c_b + 1}\right) \quad (41)$$

$$\approx S_{a22}e^{-2\gamma l}S_{b22} \quad (42)$$

$$p = S_{t21}S_{t12}(1 - e)^2 \quad (43)$$

$$\approx S_{a21}S_{a12}S_{b21}S_{b12}e^{-2\gamma l} \quad (44)$$

with l the thru or line length. The two terms in (41) yield the same quantity and their difference is an indication of the measurement error. LRM inhibits the use of (41) since only α is obtained from the match. The missing unknowns then follow from

$$e = \frac{c_a c_b}{S_{t21}S_{t12}} \quad \chi_a = \frac{c_b(1 - e)}{p} \quad \chi_b = \frac{c_a(1 - e)}{p} \quad (45)$$

with a lower accuracy compared to optimal TLR. Assuming one lossless line, ideal error boxes, and Marks' error model yields

$$\sigma_\chi^2 = \sigma_\beta^2 = \sigma_\alpha^2 = \frac{4\sigma_\delta^2}{|e^{\gamma l} - e^{-\gamma l}|^2} \quad (46)$$

$$\sigma_c^2 = 2\sigma_\delta^2 + \sigma_\alpha^2 \quad (47)$$

with σ_δ modelling the contact imperfection. Clearly, using (45) in TLR calibrations results in loss of accuracy. Its use is only justified if a high line loss invalidates the linearized error analysis of [3, eqs. 21, 37, 38].

Further error box completion requires the measurement of an equal reflect at both ports. The data S_r relates

$$S_{a22} + \frac{S_{a21}S_{a12}}{S_{r11} - \alpha_a} \approx \frac{1}{\Gamma_r e^{-2\gamma l_r}} \approx S_{b22} + \frac{S_{b21}S_{b12}}{S_{r22} - \alpha_b} \tag{48}$$

with Γ_r the standard's reflection and estimates

$$a_a = S_{r11} - \alpha_a \qquad a_b = S_{r22} - \alpha_b \tag{49}$$

$$\rho \;=\; \frac{\chi_a + 1/a_a}{\chi_b + 1/a_b} \approx \frac{S_{b21}S_{b12}}{S_{a21}S_{a12}}\,. \tag{50}$$

This measurement may be omitted if there is error box symmetry. Setting

$$a_a = \chi_b,\; a_b = \chi_a \;\Rightarrow\; a_a\chi_a = a_b\chi_b \Leftrightarrow S_{a22} = S_{b22} \tag{51}$$

forces an equal port 2 reflection.

The measurement of multiple reflects yields as many estimates ρ. Averaging this data is done via the Gauss Markov theorem. Suppose the vector $\vec{x}$ is the unknown parameter and that $\vec{y}$ is the measurement data corrupted by the correlated error $\vec{e}$. The system thus obeys

$$\vec{y} \;=\; A\vec{x} + \vec{e} \tag{52}$$

with $\vec{x}$, $\vec{e}$ and $\vec{y}$ stochastic vectors, and the property

$$E\left\{\vec{e}\right\} = \vec{0} \qquad V_{ee} = E\left\{\vec{e}\vec{e}^{+}\right\} \tag{53}$$

$$V_{xy} = V_{xx}A^{+} \qquad V_{yy} = AV_{xx}A^{+} + V_{ee} \tag{54}$$

where V is the covariance matrix. Given a realization $\vec{y}$, the conditional mean for $\vec{x}$ can be calculated. For jointly Gaussian vectors, in real and imaginary part, the result for $\vec{x}_{est} = E\left\{\vec{x}|\vec{y}\right\}$ is[7]

$$A^{+}V_{ee}^{-1}(\vec{y} - E\left\{\vec{y}\right\}) = (V_{xx}^{-1} + A^{+}V_{ee}^{-1}A)(\vec{x}_{est} - E\left\{\vec{x}\right\})\,, \tag{55}$$

using (54). The expression simplifies assuming a zero V_{xx}^{-1}, no a priori knowlegde, yielding the linear unbiased estimator

$$\vec{x}_{est} \;=\; (A^{+}V_{ee}^{-1}A)^{-1}A^{+}V_{ee}^{-1}\vec{y} \tag{56}$$

$$\;=\; F\vec{y} = E\left\{\vec{x}|\vec{y}\right\} \tag{57}$$

$$E\left\{\vec{x}_{est}|\vec{y}\right\} \;=\; FA\vec{x} + FE\left\{\vec{e}\right\} = \vec{x} \tag{58}$$

$$V_{xx|y} \;=\; E\left\{(\vec{x}_{est} - \vec{x})(\vec{x}_{est} - \vec{x})^{+}\right\} \tag{59}$$

$$\;=\; FV_{ee}F^{+} = (A^{+}V_{ee}^{-1}A)^{-1} \tag{60}$$

which is minimum variance for any error distribution, as proven in [7].

Measuring m reflects i yields m estimates

$$\rho_i(\alpha_x, \beta_x, S_{r,i}) = \frac{\chi_a + 1/a_{ai}}{\chi_b + 1/a_{bi}} \;\approx\; \rho_* + \Delta\rho_i \tag{61}$$

with ρ_* the exact zero-order value and $\Delta\rho_i = e_i$ the first-order measurement error. The unknown $\vec{x}$ in (52) is the complex ρ, and A reduces to a column of ones. The covariance matrix can be calculated for the one-line TLR case using Marks' results [3, eqs. 46, 47] for $\Delta\alpha, \Delta\beta$ and error model for the computation of $\Delta S_{r11}, \Delta S_{r22}$. A first-order series expansion allows to write (61). The result is diagonal dominant with

$$V_{ii} \propto (1 + |\Gamma_{ri}|^2)^2 \left(\frac{|\det(S_a)|^2}{|a_{a0i}|^4} + \frac{|\det(S_b)|^2}{|a_{b0i}|^4}\right) \tag{62}$$

which can be approximated using $\det(S_a) = \det(S_b)$, $|\Gamma_r| = 1$ and $a_{x0} = a_x$. The off-diagonal elements vanish if $\sigma_\alpha, \sigma_\beta$ and $\sigma_{\alpha\beta}$ are small compared to σ_a, which is true for multi-line TLR. The estimator (56) thus reduces to a weighted average with weights $1/V_{ii}$.

6 Error box normalization

The method in section 5 estimates the port 1 reflections α_a, α_b and χ_a, χ_b, p, ρ. The 7-term relative error model follows from

$$S_{a21}S_{a12} \;\approx\; k_1 = se^{\gamma l}\sqrt{\frac{p}{\rho}} \tag{63}$$

$$S_{b21}S_{b12} \;\approx\; k_2 = \rho k_1 \tag{64}$$

$$S_{a22} \;\approx\; \chi_a k_1 \tag{65}$$

$$S_{b22} \;\approx\; \chi_b k_2 \tag{66}$$

$$S_{a21}S_{b12} \;\approx\; k_3 = e^{\gamma l}S_{t21}(1 - e) \tag{67}$$

$$S_{b21}S_{a12} \;\approx\; k_4 = e^{\gamma l}S_{t12}(1 - e) \tag{68}$$

where S_{a21} is usually set to unity. The sign $s = \pm 1$ is chosen such that the recovered reflection, from (48), approximates an open or short.

The 8-term absolute error model can be recovered if the reciprocity ratio is known for the selected normalization. However, D_a and D_b can not be set freely since the ratios are related by

$$D_x = \frac{S_{x21}}{S_{x12}} \;\Rightarrow\; \frac{D_b}{D_a} \approx \frac{k_4}{k_3} \tag{69}$$

where k_4/k_3 is unity to measurement precision if both error boxes are identical in terms of reciprocity. A plausible method is to distribute the error over D_a and D_b around the expected D_s via

$$D_aD_b = D_s^2 \;\Rightarrow\; D_a \approx s_1 D_s\sqrt{k_3/k_4} \tag{70}$$

$$\Rightarrow\; S_{a21} \approx s_2\sqrt{k_1 D_a}\,. \tag{71}$$

The sign $s_i = \pm 1$ is chosen such that the obtained value approximates $e^{-j\omega\tau_i}$, where τ_i is an adaptive estimation from previous frequency points with initial value zero.

A good alternative for reciprocal error boxes is to set D_s to unity such that $D_x \approx 1$. This yields voltage normalized S-parameters, (31), if the reciprocity factor $K = 1$. The method supposes that the same renormalization at each port 2 yields a unity reciprocity ratio. Inconsistencies may arise when contacting lines on a lossy silicon substrate with different pitch probes. The transverse substrate currents[8] give an axial magnetic field, and the on-wafer modal voltage may thus depend on the probe pitch.

7 Experiment

A HP8510 network analyzer was calibrated by an on-wafer probe tip LRM calibration on a Cascade coplanar alumina substrate. The error boxes relate the raw VNA readout with the on-wafer S-parameters. A microwave test set samples the incident wave using a power splitter before the attenuator. The reflected wave is sampled using a directional coupler at the test set port. Thus, S_{x21} mainly describes the attenuator and cable loss, where S_{x12} comprises the same cable loss and the coupling coefficient. Reciprocity is clearly not valid since the forward and backward wave follow different detection paths. Nevertheless, using $D_s = 1$ in (70) allows to estimate S_{a21} if the attenuator loss, at 0 dB setting, and coupling are about the same. The deviation of D_x from unity tracks the difference in reciprocity ratio between the two test set ports, see (69) and fig. 4.

The trans-calibration LRM to TLR error boxes were computed using multi-line TLR on the same alumina substrate. These error boxes relate the LRM reference plane, at port 1 in fig. 3, to the TLR reference plane, at port 2. The normalized (26) reciprocity ratio becomes[9]

$$D_x = \frac{S_{x21}}{S_{x12}} = \frac{D_x^{TLR}}{D_x^{LRM}} = \frac{K_{x2}^{LRM}}{K_{x2}^{TLR}} \qquad (72)$$

and is unity since the modal field is quasi-TM. The reciprocity error $|D_x - 1|$ was about 10^{-4} up to 50 GHz. The cross-reflection e, see (41) and fig. 5, is high at low frequency due to a reference impedance change, a result of the non-ideal coplanar waveguide line standard. The difference between the two estimates (41), from forward and reverse measurements, indicates a repeatability error better than -40 dB. The recovered reflection of the open standard shows a slight improvement if an extra short is used via (62).

The ratios D_a, D_b and the final S_{a21} for another trans-wafer calibration are also given. The on-wafer TLR calibration was done on a lossy silicon substrate using 150 μm probes. D_a differs from unity up to 10^{-3}, which is thus the expected measurement accuracy. The difference between the estimates e, $\mathrm{dB}(e_1 - e_2)/2$, increases from -44 dB up to -32 dB at 50 GHz. The high S_{11} is due to a change in reference impedance, from the LRM 50 Ω to the coplanar waveguide line impedance. This lower accuracy might be a result of inaccurate probing. Also, the non-TM on-wafer modal field might increase the measurement's sensitivity on the probe placing.

8 Conclusion

The Lorentz reciprocity theorem, a field property, was used to derive a reciprocity ratio relating the forward and reverse transmission coefficient. The ratio depends on the characteristic impedance and a reciprocity factor. From power consistency, between the field and the macroscopic circuit parameters, follows that the factor is unity for TE or TM junctions. The characteristic impedance dependence can be removed using a suitable voltage renormalization.

An alternative TLR 7-term error box calculation sequence was presented. It is transmission coefficient based and remains valid even if an error box reflection is zero. Extensions of the algorithm include the zero- and multi-reflect case, and LRM modifications. The reciprocity condition was used to extract an absolute 8-term error model. Implicit assumptions and possible inconsistencies were demonstrated.

References

[1] R. Collin, "Foundations for Microwave Engineering," McGraw-Hill, New York, 1966.

[2] D. Williams, R. Marks, "Reciprocity Relations in Waveguide Junctions," *IEEE Transactions on Microwave Theory and Techniques,* Vol. 41, No. 6/7, June/July 1993, pp. 1105–1110.

[3] M.B. Marks, "A Multiline Method of Network Analyzer Calibration," *IEEE Transactions on Microwave Theory and Techniques,* Vol. 39, No. 7, July 1991, pp. 1205–1215.

[4] R. Pantoja, M. Howes, J. Richardson, R. Pollard, "Improved Calibration and Measurement of the Scattering Parameters of Microwave Integrated Circuits," *IEEE Transactions on Microwave Theory and Techniques,* Vol. 37, No. 11, November 1989, pp. 1675–1680.

[5] J. Brews, "Characteristic impedance of microstrip lines," *IEEE Transactions on Mi-*

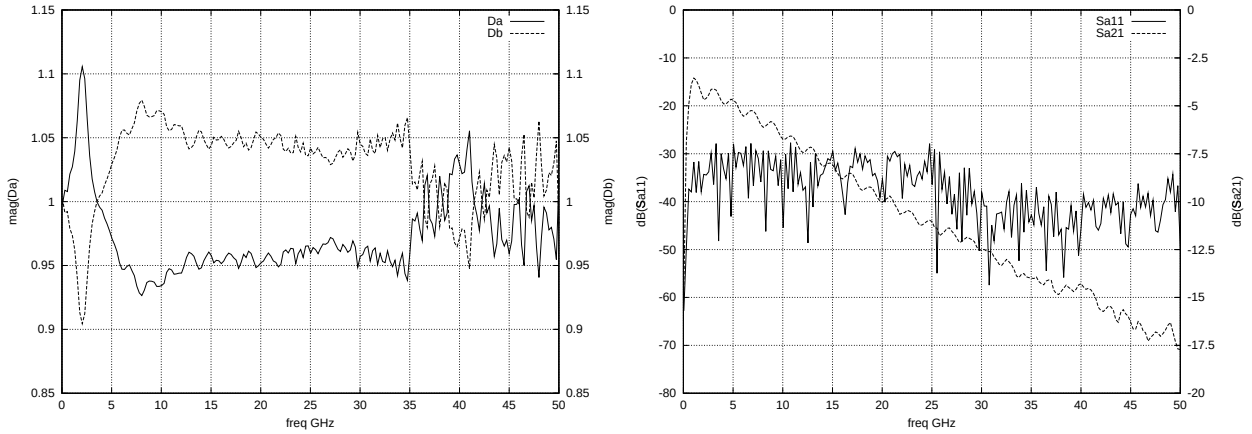

Figure 4: The ratio Da, D_b and S_{a11}, S_{a21} for a probe tip on-wafer LRM calibration. A microwave test set is not reciprocal, but assuming a unity reciprocity ratio allows for some estimate of S_{a21}. The error box consists of the test set detection circuit, the 1 m coaxial cable and the 100 μm pitch microwave probe. The reciprocity difference between the test set ports, D_b/D_a, peaks at 0.8, about -1.7 dB.

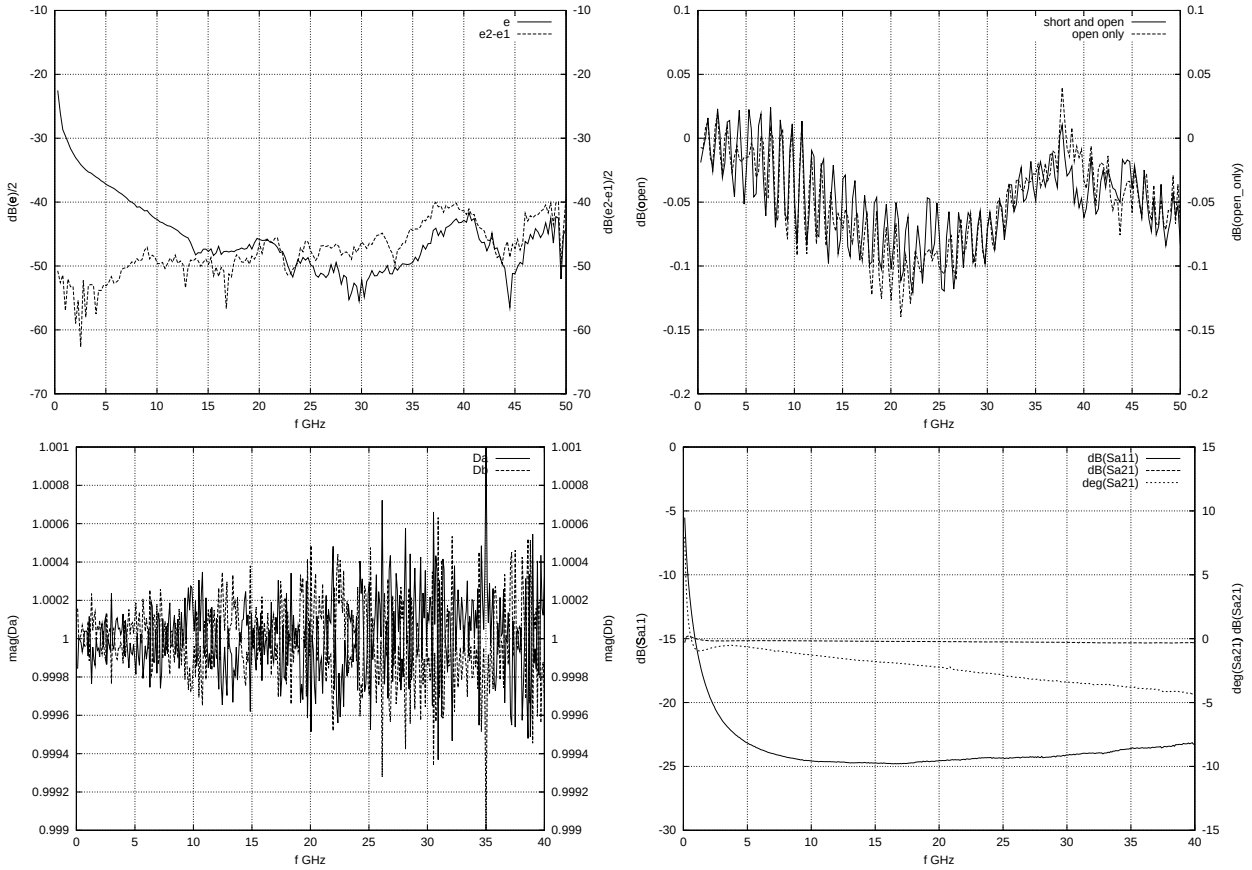

Figure 5: Top: The factor e and the difference between the two estimates, left, and the recovered reflection of an open, using the short and open calibration standard, or the open standard only. The plots are from a LRM to TLR transcalibration, both performed on an alumina calibration substrate. The 6 cpw lines, 50/25/200 μm strip/slot/ground plane, were 197.4, 432.9, 870.9, 1736.8, 1736.8, 3383.1 and 5080 μm long. Bottom: The ratio D_a, D_b and the recovered S-parameters of error box a. The plots are for a 0.5 μm thick Al 15/11/183 μm coplanar line separated from a 5 S/m Si substrate by a 1 μm thick dielectricum. LRM was used as off-wafer calibration.

crowave Theory and Techniques, Vol. 35, No. 1, Januari 1987, pp. 30–34.

[6] J. Verspecht, P. Debie, A. Barel, L. Martens, "Accurate On-Wafer Measurement of Phase and Amplitude of the Spectral Components of Incident and Scattered Voltage Waves at the Signal Ports of a Nonlinear Microwave Device," *IEEE MTT-S,* May 1995, Orlando, Florida, pp. 1029–1032.

[7] J.S. Meditch, "Probability Theory," in *Stochastic Optimal Linear Estimation and Control,* New York: McGraw-Hill, July 1969, pp. 91–95, 104, 157–167, 190–191.

[8] E. Grotelüschen, L.S. Dutta, S. Zaage, "Quasi-analytical Analysis of the Broadband Properties of Multiconductor Transmission Lines on Semiconducting Substrates," *IEEE Transactions on Components, Packaging and Manufacturing Technology–Part B,* Vol. 17, No. 3, August 1994, pp. 376–382.

[9] S. Vandenberghe, D. Schreurs, G. Carchon, B. Nauwelaers, W. De Raedt, "Characteristic Impedance Extraction Using Calibration Comparison," *IEEE Transactions on Microwave Theory and Techniques,* vol. 49, no. 12, December 2001, pp. 2573–2579.